AIP | The Journal of Chemical Physics

A pure H2O isolated line-shape model based on classical molecular dynamics simulations of velocity changes and semi-classical calculations of speed-dependent collisional parameters

N. H. Ngo, H. Tran, and R. R. Gamache

Citation: J. Chem. Phys. **136**, 154310 (2012); doi: 10.1063/1.4704675
View online: http://dx.doi.org/10.1063/1.4704675
View Table of Contents: http://jcp.aip.org/resource/1/JCPSA6/v136/i15
Published by the American Institute of Physics.

THE JOURNAL OF CHEMICAL PHYSICS **136**, 154310 (2012)

A pure H_2O isolated line-shape model based on classical molecular dynamics simulations of velocity changes and semi-classical calculations of speed-dependent collisional parameters

N. H. Ngo,[1] H. Tran,[1,a)] and R. R. Gamache[2]
[1]*Laboratoire Interuniversitaire des Systèmes Atmosphériques (LISA, CNRS UMR 7583), Université Paris-Est Créteil, Université Paris Diderot, Institut Pierre-Simon Laplace, Université Paris-Est Créteil, 94010 Créteil Cedex, France*
[2]*Department of Environmental, Earth, and Atmospheric Sciences, University of Massachusetts Lowell, 265 Riverside Street, Lowell, Massachusetts 01854, USA*

(Received 22 February 2012; accepted 30 March 2012; published online 20 April 2012)

It is well known that the Voigt profile does not well describe the (measured) shapes of isolated lines. This is due to the neglect of the intermolecular collision-induced velocity changes and of the speed dependence of the collisional parameters. In this paper, we present a new line profile model for pure H_2O which takes both of these effects into account. The speed dependence of the collisional parameters has been calculated by a semi-classical method. The velocity changes have been modeled by using the Keilson-Storer collision kernel with two characteristic parameters. The latter have been deduced from classical molecular dynamics simulations which also indicate that, for pure H_2O, the correlation between velocity-changing and state-changing collisions is not negligible, a result confirmed by the analysis of measured spectra. A partially correlated speed-dependent Keilson-Storer model has thus been adopted to describe the line-shape. Comparisons between simulated spectra and measurements for four self-broadened lines in the near-infrared at various pressures show excellent agreements. © *2012 American Institute of Physics*. [http://dx.doi.org/10.1063/1.4704675]

I. INTRODUCTION

Non-Voigt signatures on the shapes of collisionally isolated lines of water vapor have been the subject of numerous experimental and theoretical studies.[1–25] It is now well known that both the Dicke narrowing (due to collision-induced velocity changes[26]) and the speed dependence of the collisional parameters contribute to the line-shape. However, these effects have been always taken into account through simplified theoretical approaches with empirical parameters thus making the extrapolation for other spectral regions and/or experimental conditions hazardous. Indeed, most studies devoted to H_2O line profiles have used either the hard-[27,28] or soft-collision[29] approximation to describe the velocity changes narrowing effect. The resulting models are characterized by the velocity-changing (VC) collision frequency (ν_{VC}) which is related to the mass diffusion coefficient of the considered system. For the speed dependence of the line-broadening and (eventually) line-shifting coefficients, a quadratic law vs the absolute speed or a polynomial law vs the relative speed were always used. Thanks to very high signal-to-noise measurements, some studies have demonstrated the limits of these models. Reference 19, for example, shows that the soft- and hard-collision models, although they closely fit the shape of a H_2O line perturbed by N_2, lead to unrealistic nonlinearities of the retrieved ν_{VC} versus pressure. This demonstrated that the effects of speed dependence must be taken into account. This dependence was then added, through a polynomial law vs the relative speed, within the hard-collision and billiard-ball[30,31] models.[19] While the obtained value of ν_{VC} then varied linearly with pressure, it was about 40% smaller than expected from the diffusion coefficient.[19] This problem was attributed not only to the correlation between velocity- and state-changing collisions but also to the oversimplified description of the speed dependence. A consistent and physically based model is thus still needed to correctly describe the line-shape of water vapor.

In Ref. 20, the Keilson and Storer (KS) (Ref. 32) function was used, in order to model the collision-induced velocity changes for the H_2O/N_2 system, where the velocity orientation and velocity modulus changes were distinctly considered. The speed dependences of the line-broadening and line-shifting coefficients were predicted by semi-classical calculations.[18,33] With two adjustable parameters to describe the velocity (orientation and modulus) changes, several lines of H_2O measured in the ν_3 band region were correctly reproduced in a broad pressure range. The KS function was also successfully applied to pure H_2 (Ref. 34) and to H_2 diluted in Ar and N_2 (Refs. 35–39) systems for which velocity effects strongly affect the line-shape. Furthermore, it was shown that the parameters of the KS model can be (independently) determined from the auto-correlation functions of the velocity and of the squared speed of the molecules, computed by classical molecular dynamics simulations (CMDS).[40,41]

In this work, the KS function based on CMDS carried out for a large number of molecules is applied for the first time to pure H_2O lines at room temperature. It is shown that the relaxation time constants of the auto-correlation functions of the velocity and of the squared speed have very close values, indicating that the velocity orientation and modulus (speed)

[a)] Author to whom correspondence should be addressed. Electronic mail: ha.tran@lisa.u-pec.fr.

changes are completely correlated. A mono-parametric KS-3D model is thus adopted where a single parameter governs both of these changes. This parameter and the VC collisions frequency ν_{VC} are directly deduced from CMDS which, by the way, lead to a self-diffusion coefficient in excellent agreement with the measured value. CMDS also show that there is a partial correlation, which can be quantified, between velocity and internal state changes. Using the KS velocity kernel in the impact kinetic equation which includes the Doppler effect, the speed dependences of the line-broadening and line-shifting coefficients, and a partial correlation between velocity- and state-changing collisions, the line profile is then derived. Note that the speed dependences of the collisional parameters are independently calculated by a semi-classical approach. Spectra of 4 lines of pure H_2O in the near-infrared, measured with a tunable diode laser at room temperature and various pressures, are used to test the proposed model. For each transition, two adjustable parameters (one for the scaling of the speed dependence of the line-broadening and another for the correlation) are used. Their values are deduced from the comparison of measurement and calculation at only one pressure for each considered line. Comparisons between measured spectra and calculations then show very good agreements for all lines and pressures.

This paper is organized as follows: Section II presents the general equations yielding the spectral shape together with the KS model for the velocity changes and semi-classical calculations for the speed-dependent collisional parameters. Section III is devoted to the classical molecular dynamics simulations. Comparisons between measurements and calculations using the proposed model are presented and discussed in Sec. IV. Concluding remarks are given in Sec. V.

II. SPECTRAL SHAPE FROM THE KINETIC EQUATION

The normalized spectral profile $I(\omega)$ of an isolated line is given by the Laplace transform of the auto-correlation function $\bar{d}(t)$ of the tensor (here the dipole) responsible for the considered line,[42] i.e.:

$$I(\omega) = \frac{1}{\pi} \mathrm{Re}\left[\int_0^{+\infty} dt e^{i(\omega-\omega_0)t} \bar{d}(t)\right], \tag{1}$$

where ω_0 is the unperturbed angular frequency of the optical transition and $\bar{d}(t) = \int d(\vec{v}, t) d\vec{v}$ with $\vec{v}$ being the radiator velocity.

If we assume that velocity- and state-changing (dephasing) collisions are statistically uncorrelated (i.e. occurring in different collisions), the kinetic equation for $d(\vec{v}, t)$ is[27,34–36]

$$\begin{aligned}\frac{\partial}{\partial t} d(\vec{v}, t) = &-\left[\int F(\vec{v}', \vec{v}) d\vec{v}'\right] d(\vec{v}, t) \\ &+ \int F(\vec{v}, \vec{v}') d(\vec{v}', t) d\vec{v}' \\ &- [i\vec{k}.\vec{v} + \Gamma(v) + i\Delta(v)] d(\vec{v}, t).\end{aligned} \tag{2}$$

If, on the opposite, the internal state and translational velocity changes are simultaneously produced during the same collisions and thus are fully correlated, from Ref. 27 one can write

$$\begin{aligned}\frac{\partial}{\partial t} d(\vec{v}, t) = &-\left[\int F(\vec{v}', \vec{v}) d\vec{v}'\right] d(\vec{v}, t) \\ &+ \int F(\vec{v}, \vec{v}') d(\vec{v}', t) d\vec{v}' - i\vec{k}.\vec{v} d(\vec{v}, t) \\ &- [\Gamma(v) + i\Delta(v)] \frac{\int F(\vec{v}, \vec{v}') d(\vec{v}', t) d\vec{v}'}{\int F(\vec{v}', \vec{v}) d\vec{v}'}.\end{aligned} \tag{3}$$

Finally, if there is a partial correlation between velocity-changing and dephasing collisions, the resulting equation is a linear combination of Eqs. (2) and (3).[27]

The initial condition of $d(\vec{v}, t)$ is

$$d(\vec{v}, 0) = f_{MB}(\vec{v}) = \left(\frac{1}{\tilde{v}^2 \pi}\right)^{3/2} \exp\left\{-\left(\frac{\|\vec{v}\|}{\tilde{v}}\right)^2\right\}, \tag{4}$$

where $f_{MB}(\vec{v})$ is the Maxwell-Boltzmann distribution of $\vec{v}$, $\tilde{v} = \sqrt{2k_B T/m}$ is the most probable speed with m being the radiator mass.

In Eqs. (2) and (3), the velocity changes kernel $F(\vec{v}', \vec{v}) d\vec{v} d\vec{v}'$ means the probability, per unit time, of a velocity change from $\vec{v}$ (within a small $d\vec{v}$ volume) to $\vec{v}'$ (within a small $d\vec{v}'$ volume). The term $(i\vec{k}.\vec{v})$ represents the dephasing due to the Doppler effect, $\vec{k}$ being the wave vector. Finally, $\Gamma(v)$ and $\Delta(v)$ denote to the speed-dependent collisional width and shift of the optical transition [$\Gamma(v) = P\gamma(v)$ and $\Delta(v) = P\delta(v)$, P being the pressure].

A. The Keilson-Storer model for collision-induced velocity changes

Within the KS model, the velocity changes kernel $F(\vec{v}', \vec{v})$ [Eqs. (2) and (3)] is given by[32,36]

$$F(\vec{v}', \vec{v}) = \nu_{VC} f_{KS}(\vec{v}', \vec{v}) = \nu_{VC} \frac{1}{(1-\alpha^2)^{3/2}} f_{MB}\left(\frac{\vec{v}' - \alpha\vec{v}}{\sqrt{1-\alpha^2}}\right), \tag{5}$$

where $\nu_{VC} = \int F(\vec{v}', \vec{v}) d\vec{v}'$ is the frequency of velocity-changing collisions, assumed independent of $\vec{v}$ [note that $\int f_{KS}(\vec{v}', \vec{v}) d\vec{v}' = 1$]. α is a memory parameter ($0 \leq \alpha \leq 1$),[35,36] characterizing the velocity changes. For $\alpha = 0$, $f_{KS}(\vec{v}', \vec{v})$ is the Boltzmann distribution of $\vec{v}'$, a case corresponding to the hard-collisions limit[27,28] where the radiator velocity is thermalized after each collision and its memory is completely lost. If α is close to 1 (i.e., soft-collision limit,[29]), the velocity is only slightly changed after each collision and the outgoing velocity remains correlated to the incoming one for a time much greater than the interval between successive collisions. Using the KS kernel and assuming that phase and velocity changes occur in different collisions (uncorrelated), the time evolution of $d(\vec{v}, t)$ becomes, from Eq. (2):

$$\begin{aligned}\frac{\partial}{\partial t} d(\vec{v}, t) = &-\nu_{VC}\left[d(\vec{v}, t) - \int f_{KS}(\vec{v}, \vec{v}') d(\vec{v}', t) d\vec{v}'\right] \\ &- [i\vec{k}.\vec{v} + \Gamma(v) + i\Delta(v)] d(\vec{v}, t),\end{aligned} \tag{6}$$

while for a completely correlated situation, from Eq. (3) one gets

$$\frac{\partial}{\partial t}d(\vec{v},t) = -\nu_{VC}\left[d(\vec{v},t) - \int f_{KS}(\vec{v},\vec{v}')d(\vec{v}',t)d\vec{v}'\right] - i\vec{k}.\vec{v}d(\vec{v},t) - [\Gamma(v)+i\Delta(v)] \times \int f_{KS}(\vec{v},\vec{v}')d(\vec{v}',t)d\vec{v}'. \quad (7)$$

In the intermediate situation of a partial correlation between velocity and internal state changes, a linear combination of Eqs. (6) and (7) must be used.[27] Denoting as η the correlation parameter, the kinetic equation becomes

$$\frac{\partial}{\partial t}d(\vec{v},t) = -[\nu_{VC} - \eta\{\Gamma(v)+i\Delta(v)\}]\,d(\vec{v},t) + [\nu_{VC} - \eta\{\Gamma(v)+i\Delta(v)\}] \times \int f_{KS}(\vec{v},\vec{v}')d(\vec{v}',t)d\vec{v}' - [i\vec{k}\vec{v} + \Gamma(v) + i\Delta(v)]d(\vec{v},t) \quad (8)$$

with the obvious two limits: $\eta = 0$ for no correlation [Eq. (6)] and $\eta = 1$ for the fully correlated model [Eq. (7)]. Note that Eq. (8) is obtained by substituting a speed-dependent VC frequency $\tilde{\nu}_{VC}(v)$ to ν_{VC} into Eq. (6) with

$$\tilde{\nu}_{VC}(v) = \nu_{VC} - \eta\{\Gamma(v)+i\Delta(v)\}. \quad (9)$$

Several limiting cases can be derived from Eqs. (5) and (8). For $\eta \neq 0$, $\alpha \to 0$ and $\alpha \to 1$ correspond to the partially correlated speed-dependent hard- and soft-collisions models,[27,43] respectively. These then become the speed-dependent hard- and soft-collision models when $\eta = 0$. For $\nu_{VC} = 0$, $\eta = 0$ the speed-dependent Voigt model is obtained and, if $\nu_{VC} = 0$, $\eta = 0$ and no speed dependence is assumed, the line-shape is the usual Voigt model.

B. Speed dependences of the collisional parameters

The semi-classical Robert-Bonamy theory[44] in its complex form (CRB) was used to predict the speed dependences of the collision parameters. Within this approach, the half-width and line shift for a transition f ← i and a given relative speed v_{rel} can be written in terms of the optical cross sections σ_{Re} and σ_{Im}:

$$\gamma_{f\leftarrow i}(v_{rel}) + i\delta_{f\leftarrow i}(v_{rel}) = \frac{n_2}{2\pi c}\sum_{J_2}\langle J_2|\,\rho_2\,|J_2\rangle\, v_{rel}[\sigma_{Re}(J_2,v_{rel}) + i\sigma_{Im}(J_2,v_{rel})], \quad (10)$$

where all quantities are real. ρ_2 and n_2 are the density operator (its matrix element giving the relative population) and number density of perturbers. Note, here J_2 labels the state of the perturbing molecule, here defined by J K_a K_c. The optical cross section is given by

$$\sigma_{Re}(J_2,v_{rel}) + i\sigma_{Im}(J_2,v_{rel}) = \int_0^\infty 2\pi b\,[1 - [\cos\{S_1+\mathrm{Im}(S_2)\} - i\sin\{S_1+\mathrm{Im}(S_2)\}]\,e^{-Re(S_2)}]db, \quad (11)$$

where b is the impact parameter and S_1 and S_2 are the first and second order terms in the successive expansion of the Liouville scattering matrix S. S_1 and S_2 depend on the ro-vibrational states involved and the associated collision-induced jumps from these levels, on the intermolecular potential and characteristics of the collision dynamics. Within the semi-classical CRB formalism, the S_2 terms can be written as the product of reduced matrix elements (quantum mechanical component) for the perturber and the radiator (here the same, H_2O) and the resonances functions (classical component). The exact forms of these terms can be found in Refs. 45–47.

The intermolecular potential used in the calculations is a sum of an electrostatic component (dipole and quadrupole moments of H_2O), an atom-atom component expanded to 20th order and rank = 4 for the radiator and perturber, and an isotropic induction and a London dispersion potential. Many of the molecular parameters for the H_2O–H_2O system are well known and the present calculations use the best available values from the literature.[48–51] The atom-atom parameters were determined from the heteronuclear parameters of Bouanich[52] and the combination rules of Hirschfelder *et al.*[53] (see Ref. 54 for specific details and parameter values).

The wavefunctions used to evaluate the reduced matrix elements are obtained by diagonalizing the Watson Hamiltonian[55] in a symmetric top basis. The wavefunctions for the ground vibrational state are determined using the constants of Matsushima *et al.*[56] and those for the $2v_1 + v_2 + v_3$ state use the ν_3 constants from Flaud and Camy-Peyret[57] to give wavefunctions with proper symmetry.

Calculations of the broadening and shifting coefficients vs the relative speed v_{rel} were made for the four transitions in the $2\nu_1 + \nu_2 + \nu_3$ band of H_2O listed in Table I. They were carried out for 35 values of v_{rel} from 217 m/s to 7967 m/s for all levels of the perturber (H_2O) up to J = 10. The broadening and shifting vs the absolute speed were then obtained from a Maxwell Boltzmann average over the perturber velocity $\vec{v}_p$ by (see Appendix D of Ref. 34):

$$\gamma(v) + i\delta(v) = \frac{1}{\tilde{v}_p}\frac{2}{\sqrt{\pi}}\int_0^\infty dv_{rel}[\gamma(v_{rel}) + i\delta(v_{rel})]\frac{v_{rel}}{v}\sinh \times \left[\frac{2vv_{rel}}{\tilde{v}_p}\right]\exp\left[-\frac{v^2+v_{rel}^2}{\tilde{v}_p}\right]. \quad (12)$$

TABLE I. The correlation parameter η and the A factor applied to the input (CRB calculated, see Sec. II B) speed-dependent line-broadening coefficient, for the considered $2\nu_1 + \nu_2 + \nu_3$ band transitions.

Position (cm^{-1})	J′ Ka′ Kc′	J″ Ka″ Kc″	E (cm^{-1})	η	A
11 988.4939	6 0 6	7 0 7	586.2436	0.211	1.087
12 236.5601	5 1 5	4 1 4	224.8384	0.258	1.086
12 249.3895	6 0 6	5 0 5	325.3479	0.247	1.042
12 280.6634	7 2 6	6 2 5	552.9114	0.270	1.034

III. CLASSICAL MOLECULAR DYNAMICS SIMULATIONS

As demonstrated in Refs. 34, 40, and 41, the KS parameters ν_{VC} and α can be deduced from independent calculations of the auto-correlation functions of the center of mass velocity $\phi_{\vec{v}}(t)$ and of the squared speed (i.e., the energy) $\phi_{v^2}(t)$. Indeed, from Eq. (5), these are given by[41]

$$\begin{aligned}\phi_{\vec{v}}(t) &= \frac{3}{2}\tilde{v}^2\exp\{-t[\nu_{VC}(1-\alpha)]\},\\ \phi_{v^2}(t) &= \frac{9}{4}\tilde{v}^4 + \frac{6}{4}\tilde{v}^4\exp\{-t[\nu_{VC}(1-\alpha^2)]\}.\end{aligned} \qquad (13)$$

CMDS were thus performed, for 5×10^6 H_2O molecules at 296 K, using the pairwise site-site potential given in Ref. 58. Detailed description of these simulations can be found in Ref. 59. The molecules were in 250 cubic boxes (each containing 20 000 molecules) with periodic boundary conditions, treated in parallel on an IBM Blue Gene/P computer. The size of each box is deduced through the perfect gas law from the number of molecules, temperature, and density. The center of mass position and velocity, the orientation, and the angular momentum of each molecule were initialized according to the Maxwell-Boltzmann statistics. Quaternion coordinates were used to treat the rotation of the molecules.[60] After several tests, a temporization time[60,61] of about 20 ps and a time step of 1 fs were retained. During CMDS, the parameters (center of mass position, velocity, angular momentum, and molecular orientation) describing the classical state of each molecule are computed for each time step. The auto-correlation functions of the center of mass velocity and of the squared speed are then obtained from

$$\begin{aligned}\phi_{\vec{v}}(t) &= \langle\vec{v}(t).\vec{v}(0)\rangle = \frac{1}{N}\sum_{i=1,N}\vec{v}_i(t).\vec{v}_i(0),\\ \phi_{v^2}(t) &= \langle v^2(t).v^2(0)\rangle = \frac{1}{N}\sum_{i=1,N}v_i^2(t).v_i^2(0),\end{aligned} \qquad (14)$$

where N is the number of molecules treated. Figure 1 shows the obtained CMDS auto-correlation functions $\phi_{\vec{v}}(t)$ and $\phi_{v^2}(t)$ and the expected $t \to 0$ and $t \to +\infty$ limits given by Eq. (13). The time constants deduced from their adjustment using exponential decay functions (leading to very good fits, see Fig. 1) are, respectively, $\tau_{\vec{v}} = 118.96$ and $\tau_{v^2} = 101.25$ ps for $T = 296$ K and 1 atm. Note that this value of $\tau_{\vec{v}}$ leads to a diffusion coefficient $[D = \tau_{\vec{v}}(k_BT)/m]$ at 296 K and 1 atm of $D = 0.164$ cm^2 s^{-1}, in excellent agreement with the measured value of 0.17 cm^2 s^{-1} at 300 K of Ref. 62.

Note that the fact that $\tau_{\vec{v}}$ and τ_{v^2} have very close values validates the use of a unique memory parameter α in the KS kernel (thus the mono-parametric KS model) to describe the changes of both the velocity modulus and orientation.[34] The situation here is thus similar to pure H_2 system,[41] but different from the cases of H_2/Ar and H_2/N_2,[36,38,39] for example, where $\tau_{\vec{v}}$ is much smaller than τ_{v^2} and a bi-parametric model must be used to distinctly describe the velocity orientation and modulus changes. From the values of $\tau_{\vec{v}}$, τ_{v^2}, and Eq. (13), one obtains $\alpha = \tau_{\vec{v}}/\tau_{v^2} - 1 = 0.17$ and $\nu_{VC} = \tau_{v^2}/[\tau_{\vec{v}}(2\tau_{v^2} - \tau_{\vec{v}})]$ $= \frac{1}{98.15}$ ps^{-1} (or 0.054 cm^{-1}) at 1 atm. Note that at pressures considered in this work, collisions are essentially binary and ν_{VC} is thus proportional to the pressure.

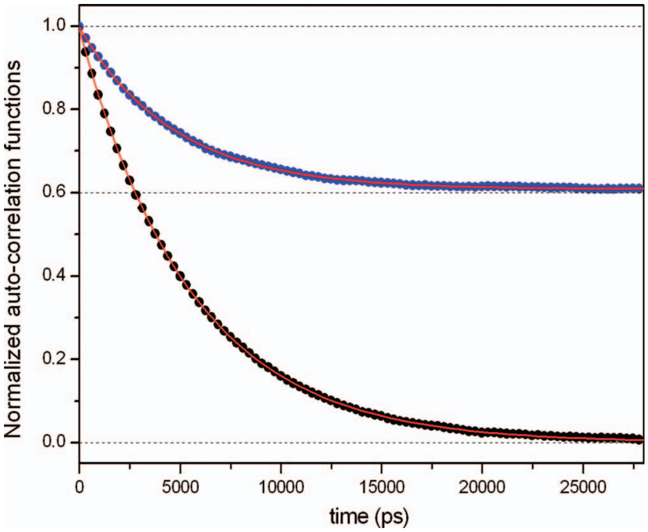

FIG. 1. The normalized (to the theoretical initial values at $t \to 0$ given by Eq. (13)) auto-correlation functions of the center of mass velocity $\phi_{\vec{v}}(t)$ (black points, all calculated points have not been plotted) and squared speed $\phi_{v^2}(t)$ (blue points), directly obtained from CMDS performed at 296 K and 0.02 amagat. The theoretical $t \to +\infty$ and $t \to 0$ limits [Eq. (13)] are indicated by the black dashed lines and the exponential fits by the red lines.

CMDS were also used to get information on the degree of correlation between velocity- and state-changing collisions. This was achieved by considering $\sum_i N_M(v_i, \omega_k, 0)$ —the sum over all speeds of the number of molecules which have the translational and angular speeds v_i (within a small interval Δv) and ω_k (within a small interval $\Delta\omega$) at the initial time $t = 0$. We then extract from CMDS three numbers: $\sum_i N_M(v_i, \omega_k, t)$ with $N_M(v_i, \omega_k, t)$—the number of molecules among $N_M(v_i, \omega_k, 0)$ which have both translational and angular speeds unchanged at time t; $\sum_i N_M(v_i, t)$ with $N_M(v_i, t)$—the number of molecules among $N_M(v_i, \omega_k, 0)$ which have v unchanged at time t regardless of their angular speed; and $\sum_i N_M(\omega_k, t)$ with $N_M(\omega_k, t)$—the number of molecules among $N_M(v_i, \omega_k, 0)$ which have ω unchanged at time t regardless of their translational velocity. The time dependence of $\sum_i N_M(v_i, \omega_k, t)$ reflects how collisions change both the speed and angular momentum while that of $\sum_i N_M(v_i, t)$ [resp. $\sum_i N_M(\omega_k, t)$] is associated with speed [resp. angular momentum] changes only. Comparing the first number to the product of the last two thus enables a study of correlation since, for a completely uncorrelated case, these should be equal. Figure 2 shows two examples of the time evolutions of $\sum_i N_M(v_i, \omega_k, t)$, $\sum_i N_M(v_i, t)$, and $\sum_i N_M(\omega_k, t)$. For the two cases, the time evolutions of $\sum_i N_M(v_i, t)$ and $\sum_i N_M(\omega_k, t)$ are different, indicating that the translational speed and angular momentum changes are not fully correlated. However, $\sum_i N_M(v_i, \omega_k, t)$ (black curves) is different from the product of $\sum_i N_M(v_i, t)$ and $\sum_i N_M(\omega_k, t)$ (grey curves), thus demonstrating a partial correlation between the velocity-changing and dephasing collisions.

Using Eq. (9), the value of the correlation parameter η can be deduced as follows: The relaxation times τ_v and τ_ω of

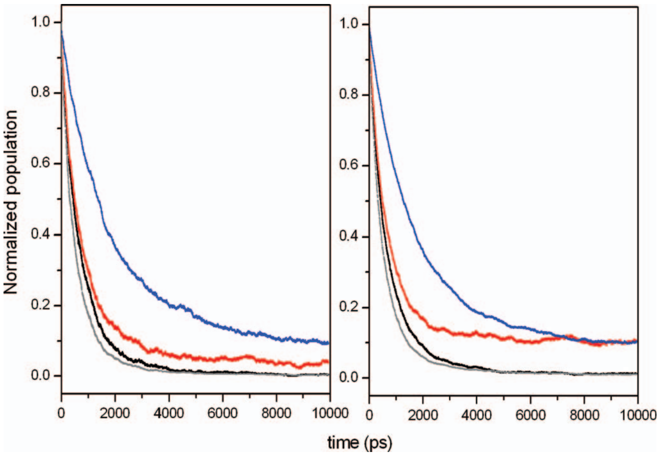

FIG. 2. Normalized population [divided by the total initial number of molecules $\sum_i N_M(v_i, \omega_k, 0)$] directly obtained from CMDS: in black is $\sum_i N_M(v_i, \omega_k, t)$; in red is $\sum_i N_M(\omega_k, t)$, and in blue is $\sum_i N_M(v_i, t)$ (see text). The left and right panels display the result obtained for the rotational energy $E_{rot} = 585.58\ cm^{-1}$ and $E_{rot} = 277.69\ cm^{-1}$, respectively. The grey curves are the product of the red and blue ones $[\sum_i N_M(\omega_k, t).\sum_i N_M(v_i, t)]$.

$\sum_i N_M(v_i, t)$ and $\sum_i N_M(\omega_k, t)$ are directly related to ν_{VC} and Γ, respectively. If there is no correlation between velocity-changing and dephasing collisions, the relaxation time of $\sum_i N_M(v_i, t).\sum_i N_M(\omega_k, t)$ [the grey curves] would be $\tau_{NC} = (\tau_v.\tau_\omega)/(\tau_v + \tau_\omega)$. If there is a partial correlation, from Eq. (9), the relaxation time of $\sum_i N_M(v_i, \omega_k, t)$ [the black curves] is $\tau_{pC} = (\tilde{\tau}_v.\tau_\omega)/(\tilde{\tau}_v + \tau_\omega) = (\tau_v.\tau_\omega)/[\tau_\omega + (1 - \eta)\tau_v]$. The value of η is thus given by $\eta = \frac{\tau_\omega + \tau_v}{\tau_v}[1 - \frac{\tau_{NC}}{\tau_{pC}}]$. From this equation and the values of τ_v, τ_ω, and τ_{pC} determined from exponential fits of $\sum_i N_M(v_i, t)$, $\sum_i N_M(\omega_k, t)$, and $\sum_i N_M(v_i, \omega_k, t)$, respectively, one can thus determine the value of η. For the two examples of Fig. 2, we obtain $\eta = 0.22$ and 0.25 for Figs. 2(a) and 2(b), respectively.

IV. COMPUTATIONAL PROCEDURE AND COMPARISON BETWEEN MODEL AND EXPERIMENT

Measured spectra of 4 $2\nu_1 + \nu_2 + \nu_3$ band lines of pure H_2O in the near-infrared were used to test the developed model. These measurements[25] were performed at room temperature and for various pressures using a tunable diode-laser system.

A. Computational procedure

A purely numerical method, described in Ref. 34, was used to calculate the line profile $I(\omega)$ using Eqs. (1), (4), (5) and (8). The speed and orientation (relative to the light propagation wave vector direction) of the velocity $\vec{v}$ are discretized onto separate grids and one then solves a set of differential equations providing the time evolutions of the various projections of $d(\vec{v}, t)$ onto the speed and orientation grids. After several convergence tests, 40 discrete values for both the speed and orientation were retained, thus leading to 1600 couples. Recall that the values of ν_{VC} and α were determined from CMDS (cf. Sec. III) and then have fixed values in all calculations. The speed dependences of the line-broadening and line-shifting coefficients were predicted using the semi-classical CRB method (cf. Sec. II B). As shown in Sec. III, a partial correlation between velocity- and state-changing collisions is needed to correctly describe the time evolution of the system, and thus the line-shape. For the four lines considered here (see Table I) their initial level rotational energy varies from 220 to 590 cm^{-1} and the corresponding values of η determined from CMDS varies from 0.30 to 0.22. However, these values are approximate since the limited number of molecule treated in the CMDS does not ensure fully converged statistics (e.g., the remaining "noise" on the curves in Fig. 2). Furthermore, an accurate determination of η for each line would require a correct requantization of the classical rotational energy,[63] a complicated problem for an asymmetric-top molecule. Hence, in the following, the value of η was re-determined from fits of measured spectra. Finally, as done in Ref. 20, an amplitude scaling factor (A) was applied to the input (cf. Sec. II B) speed-dependent line-broadening coefficient $\gamma(v)$ in order to fit the measured profile, while no scaling factor was used for the speed-dependent line-shifting $\delta(v)$. The speed-dependent collisional width [Eq. (8)] thus becomes $\Gamma(v) = P[A\gamma(v)]$. This factors A and η were determined for each line, from the best agreement between the measured spectrum at the highest pressure and the corresponding simulated spectrum, leading to the values given in Table I. It is worth noting that the values of η retrieved from the measured line-shapes, as explained just above, range from 0.211 to 0.270 and are thus in good agreement with the completely independent CMDS predictions.

B. Comparisons between measured and calculated spectra

The values of η and A being known and then fixed, comparisons between experiments and calculations can now be made for different pressures. The model will be denoted pCSDKS (for partial correlated speed-dependent Keilson-Storer) from now on. Because of the complexity of the line profile calculations, direct fits of measured spectra by the model are extremely difficult to implement and were not performed. The experiment/model comparisons were thus made by considering the results of the fits of both measured and calculated spectra by Voigt profiles, as done in Ref. 20, allowing an indirect but meaningful test of the model. Examples of the results, presented in Fig. 3, show excellent agreement for both the amplitude and the shape of the residuals. Note that the (slight) asymmetry of the measured profile is correctly reproduced by the model, regardless of the considered pressure. This asymmetry, larger for heavier collision partner,[6] is the signature of the speed dependence of the line shift.

In order to give an overall view of non-Voigt effects by showing how well the model takes them into account for all considered lines, the amplitude of the W signature in the residuals (e.g., Fig. 3) normalized by the absorption peak, and the line-broadening coefficient Γ/P_{H2O} are considered (as done in Ref. 20) and plotted in Figs. 4 and 5. The error bars on the experimentally determined values of W and Γ were

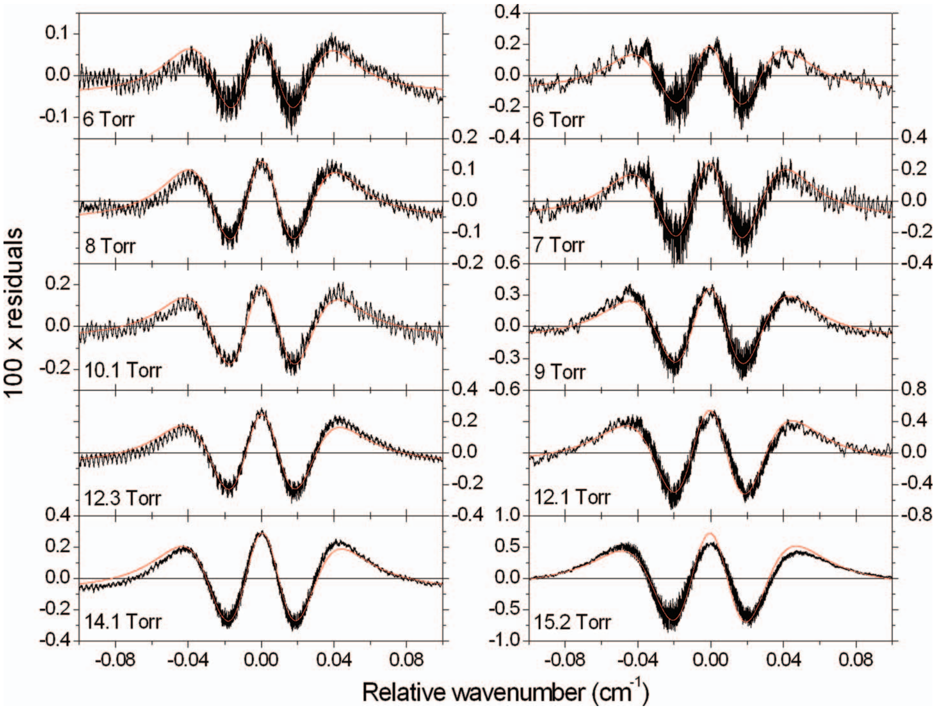

FIG. 3. Comparisons between residuals obtained from fits by Voigt profiles of measured spectra (black) and of those calculated for the same pressure conditions using the present pCSDKS model (red). The results are for the 6 0 6 ← 7 0 7 (left) and 5 1 5 ← 4 1 4 (right) lines of pure H_2O, at room temperature and various pressures (indicated on the plots).

derived from the scatter of results obtained from different spectra (from 2 to 4) measured at the same pressure. Good agreements between measured and calculated values are obtained for both W and Γ.

In order to show the evolutions of Γ/P and W from the Doppler to the collisional regimes, simulations with the pCSDKS model have been performed for a large range of pressure and fitted with a Voigt profile. The values obtained of W and Γ/P versus Γ/Γ_D with Γ_D being the Doppler broadening are exemplified in Fig. 6. As observed in Fig. 6 and previously for H_2O/N_2,[20] Γ/P increases with Γ/Γ_D at low values of Γ/Γ_D and then becomes constant at high values of Γ/Γ_D, in the collisional regime. For W, its magnitude increases with Γ/Γ_D when $\Gamma/\Gamma_D \rightarrow \approx 1$ and then decreases and becomes constant at high values of Γ/Γ_D. This is also consistent with what was observed for H_2O/N_2 (Fig. 6 and Ref. 20). The Γ/Γ_D range of measured spectra considered in this work being limited (cf. Fig. 6) due to the broad Doppler width and low saturation pressure, comparisons of the model with pure H_2O

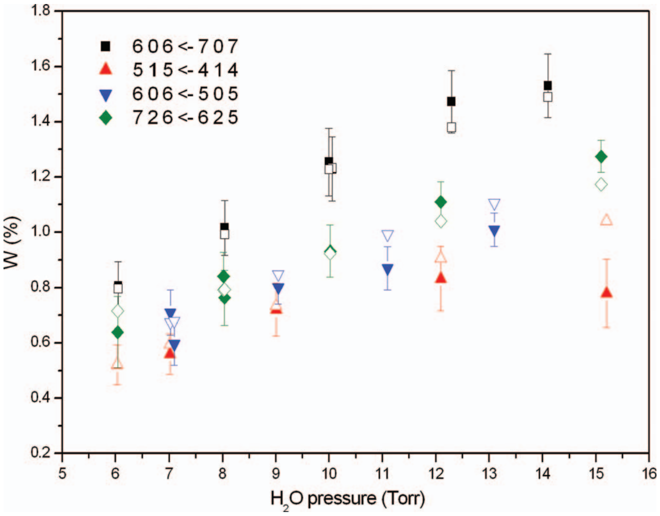

FIG. 4. Peak absorption normalized amplitude of the W signature in the residuals obtained from fits of measured (full symbols) and pCSDKS-calculated (open symbols) spectra with Voigt profiles.

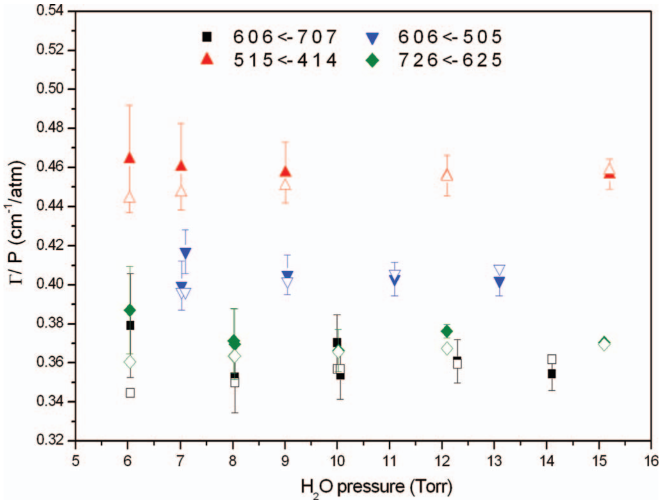

FIG. 5. The Lorentz widths obtained from fits of measured (full symbols) and pCSDKS-calculated (open symbols) spectra with Voigt profiles.

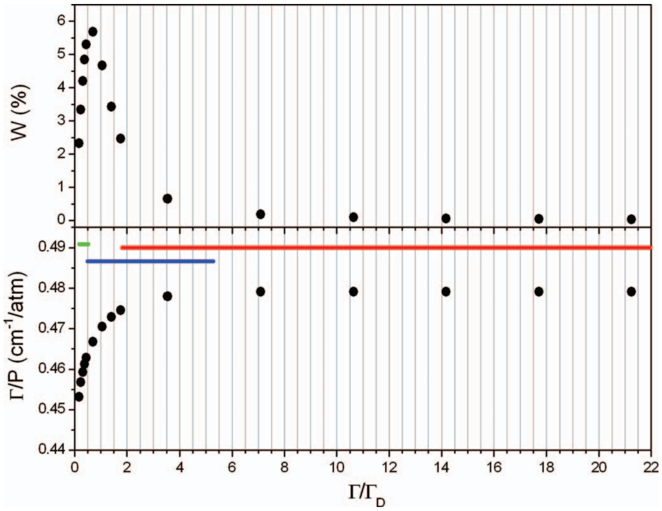

FIG. 6. Values of Γ/P and W obtained from pCSDKS calculated spectra for the 5 1 5 ← 4 1 4 line vs the ratio Γ/Γ_D. In green is the Γ/Γ_D range of the pure H_2O spectra considered in this work, in blue and red are the Γ/Γ_D ranges of the ν_3 11 1 11 ← 10 1 10 and 4 0 4 ← 3 0 3 lines of H_2O/N_2 studied in Ref. 20.

spectra measured at longer wavelengths, thus leading to a broader range of Γ/Γ_D, will be performed in the future.

V. CONCLUSIONS

A new theoretical approach has been developed to calculate the line-shape of pure H_2O. Different effects contributing to the observed deviations from the usual Voigt profile have been taken into account. The speed dependences of the collisional parameters are predicted by a semi-classical method. The influence of the collision-induced velocity changes is modeled by using the Keilson-Storer collision kernel. The parameters of this model are determined from (completely independent) classical molecular dynamics simulations. A partial correlation between velocity-changing and dephasing collisions, predicted by classical molecular dynamic simulations, is also taken into account. The final line-shape model, named pCSDKS, has been successfully tested by comparisons with diode laser measurements for 4 lines of H_2O in the near-infrared.

The proposed model is physically based and takes into account different mechanisms contributing to the line-shape. However, its complexity and the large computer cost of its use make it difficult (if not unrealistic) to use in practical applications (for atmospheric spectra calculations, for example). While these applications require very accurate spectroscopic data and line-shape description, a simple-to-use approach, compatible with line-by-line parameters databases and intensive spectra calculations, is still to be found. As mentioned in the Introduction, several simplified models have been proposed, but often not consistent and poorly physically based. The present model can thus be used to analyze and test these currently used line-shape approaches for future attempts to identify the most adapted one (i.e., that offering the best and acceptable simplicity/precision compromise). This subject is under study and will be presented in a future work.

ACKNOWLEDGMENTS

The authors from LISA thank the *Institut du Développement et des Ressources en Informatique Scientifique* (IDRIS) for giving access to the IBM Blue Gene/P parallel computer and the French program "Les Enveloppes Fluides et l'Environnement, Chimie Atmosphérique" (LEFE-CHAT) from the "Institut National des Sciences de l'Univers" (INSU) for financial support. Dr. J.-M. Hartmann is gratefully acknowledged for helpful discussions and his careful reading of this paper. R.R.G. is pleased to acknowledge support of this research by the National Science Foundation through Grant No. ATM-0803135. Any opinions, findings, and conclusions or recommendations expressed in this material are those of the author(s) and do not necessarily reflect the views of the National Science Foundation. R.R.G. is also grateful to the Paris-Est *Pôle de Recherche et d'Enseignement Supérieur* for providing a one month research scientist position at LISA in June 2011.

[1] R. S. Eng, A. R. Calawa, T. C. Harman, P. L. Kelley, and A. Javan, Appl. Phys. Lett. **21**, 303 (1972).

[2] R. S. Eng, P. L. Kelley, A. Mooradian, A. R. Calawa, and T. C. Harman, Chem. Phys. Lett. **19**, 524 (1973).

[3] R. S. Eng and A. W. Mantz, J. Mol. Spectrosc. **74**, 388 (1979).

[4] B. E. Grossmann and E. V. Browell, J. Mol. Spectrosc. **136**, 264 (1989).

[5] B. E. Grossmann and E. V. Browell, J. Mol. Spectrosc. **138**, 562 (1989).

[6] B. E. Grossmann and E. V. Browell, J. Quant. Spectrosc. Radiat. Transf. **45**, 339 (1991).

[7] T. Giesen, R. Schieder, G. Winnewisser, and K. M. T. Yamada, J. Mol. Spectrosc. **153**, 406 (1992).

[8] V. G. Avetisov, A. I. Nadezhdinskii, A. N. Khusnutdinov, P. M. Omarova, and M. V. Zyrianov, J. Mol. Spectrosc. **160**, 326 (1993).

[9] P. L. Ponsardin and E. V. Browell, J. Mol. Spectrosc. **185**, 58 (1997).

[10] V. Nagali, S. I. Chou, D. S. Baer, and R. K. Hanson, J. Quant. Spectrosc. Radiat. Transf. **57**, 795 (1997).

[11] N. Schmucker, C. Trojan, T. Giesen, R. Schieder, K. M. T. Yamada, and G. Winnewisser, J. Mol. Spectrosc. **184**, 250 (1997).

[12] R. A. Toth, J. Mol. Spectrosc. **201**, 218 (2000).

[13] C. Claveau, A. Henry, D. Hurtmans, and A. Valentin, J. Quant. Spectrosc. Radiat. Transf. **68**, 273 (2001).

[14] M. Lepère, A. Henry, A. Valentin, and C. Camy-Peyret, J. Mol. Spectrosc. **208**, 25 (2001).

[15] L. Moretti, A. Sasso, L. Gianfrani, and R. Ciurylo, J. Mol. Spectrosc. **205**, 20 (2001).

[16] C. Claveau, A. Henry, M. Lepère, A. Valentin, and D. Hurtmans, J. Mol. Spectrosc. **212**, 171 (2002).

[17] D. Lisak, G. Rusciano, and A. Sasso, J. Mol. Spectrosc. **227**, 162 (2004).

[18] G. Wagner, M. Birk, R. R. Gamache, and J. M. Hartmann, J. Quant. Spectrosc. Radiat. Transf. **92**, 211 (2005).

[19] D. Lisak, J. Hodges, and R. Ciurylo, Phys. Rev. A **73**, 012507 (2006).

[20] H. Tran, D. Bermejo, J. L. Domenech, P. Joubert, R. R. Gamache, and J. M. Hartmann, J. Quant. Spectrosc. Radiat. Transf. **108**, 126 (2007).

[21] H. Li, A. Farooq, J. B. Jeffries, and R. K. Hanson, J. Quant. Spectrosc. Radiat. Transf. **109**, 132 (2008).

[22] J. T. Hodges, D. Lisak, N. Lavrentieva, A. Bykov, L. Sinita, J. Tennyson, R. J. Barber, and R. N. Tolchenov, J. Mol. Spectrosc. **249**, 86 (2008).

[23] D. Lisak and J. T. Hodges, J. Mol. Spectrosc. **249**, 6 (2008).

[24] M. D. De Vizia, F. Rohart, A. Castrillo, E. Fasci, L. Moretti, and L. Gianfrani, Phys. Rev. A **83**, 052506 (2011).

[25] N. H. Ngo, N. Ibrahim, X. Landsheere, H. Tran, P. Chelin, M. Schwell, and J. M. Hartmann, "Intensities and shapes of H_2O lines in the near-infrared by tunable diode laser spectroscopy," J. Quant. Spectrosc. Radiat. Transf. (in press).

[26] R. H. Dicke, Phys. Rev. **89**, 472 (1953).

[27] S. G. Rautian and I. I. Sobel'man, Sov. Phys. Usp. **9**, 701 (1967).

[28] M. Nekin and A. Ghatak, Phys. Rev. **135**, A4 (1964).

[29] L. Galatry, Phys. Rev. **122**, 1218 (1961).

[30] D. A. Shapiro, R. Ciurylo, J. R. Drummond, and A. D. May, Phys. Rev. A **65**, 012501 (2001).

[31] R. Ciurylo, D. A. Shapiro, J. R. Drummond, and A. D. May, Phys. Rev. A **65**, 012502 (2001).

[32] J. Keilson and J. E. Storer, Q. Appl. Math. **10**, 243 (1952).

[33] R. R. Gamache and J. M. Hartmann, J. Quant. Spectrosc. Radiat. Transf. **83**, 119 (2004).

[34] H. Tran and J. M. Hartmann, J. Chem. Phys. **130**, 094301 (2009).

[35] D. Robert and L. Bonamy, Eur. Phys. J. D **2**, 245 (1998).

[36] L. Bonamy, H. Tran, P. Joubert, and D. Robert, Eur. Phys. J. D **31**, 459 (2004).

[37] H. Tran, P. Joubert, L. Bonamy, B. Lavorel, V. Renard, F. Chaussard, O. Faucher, and B. Sinardet, J. Chem. Phys. **122**, 194317 (2005).

[38] H. Tran, F. Chaussard, N. Le Cong, B. Lavorel, O. Faucher, and P. Joubert, J. Chem. Phys. **131**, 174310 (2009).

[39] H. Tran, F. Thibault, and J. M. Hartmann, J. Quant. Spectrosc. Radiat. Transf. **112**, 1035 (2011).

[40] P. Joubert, P. N. M. Hoang, L. Bonamy, and D. Robert, Phys. Rev. A **66**, 042508 (2002).

[41] H. Tran, J. M. Hartmann, F. Chaussard, and M. Gupta, J. Chem. Phys. **131**, 154303 (2009).

[42] J. M. Hartmann, C. Boulet, and D. Robert, *Collisional Effects on Molecular Spectra. Laboratory Experiments and Models, Consequences for Applications* (Elsevier, Amsterdam, 2008).

[43] A. S. Pine, J. Quant. Spectrosc. Radiat. Transf. **62**, 397 (1999).

[44] D. Robert and J. Bonamy, J. Phys. France **40**, 923 (1979).

[45] R. Lynch, "Half-widths and line shifts of water vapor perturbed by both nitrogen and oxygen," Ph.D. dissertation, Physics Department, University of Massachusetts Lowell, 1995.

[46] R. R. Gamache, R. Lynch, and S. P. Neshyba, J. Quant. Spectrosc. Radiat. Transf. **59**, 319 (1998).

[47] R. Lynch, R. R. Gamache, and S. P. Neshyba, J. Quant. Spectrosc. Radiat. Transf. **59**, 595 (1998).

[48] S. L. Shostak and J. S. Muenter, J. Chem. Phys. **94**, 5883 (1991).

[49] W. H. Flygare and R. C. Benson, Mol. Phys. **20**, 225 (1971).

[50] Y. Luo, H. Agren, O. Vahtras, P. Jorgensen, V. Spirko, and H. Hettema, J. Chem. Phys. **98**, 7159 (1993).

[51] D. R. Lide, *CRC Handbook of Physics and Chemistry*, 83rd ed. (The Chemical Rubber Company, Cleveland, OH, 2003).

[52] J. P. Bouanich, J. Quant. Spectrosc. Radiat. Transf. **47**, 243 (1992).

[53] J. O. Hirschfelder, C. F. Curtiss, and R. B. Bird, *Molecular Theory of Gases and Liquids* (Wiley, New York, 1964).

[54] B. K. Antony, S. Neshyba, and R. Gamache, J. Quant. Spectrosc. Radiat. Transf. **105**, 148 (2007).

[55] J. K. G. Watson, J. Chem. Phys. **46**, 1935 (1967).

[56] F. Matsushima, H. Odashima, T. Iwaskai, and S. Tsunekawa, J. Mol. Struct. **352-353**, 371 (1995).

[57] J. M. Flaud and C. Camy-Peyret, private communication (2005).

[58] E. M. Mas, R. Bukowski, K. Szalewicz, G. C. Groenenboom, P. E. S. Wormer PES, and Ad van derAvoird, J. Chem. Phys. **113**, 6687 (2000).

[59] H. Tran, "Diffusion coefficient, broadening coefficient and collision induced absorption and the far wing of the rotational band of water vapor by classical molecular dynamics simulations" (unpublished).

[60] M. P. Allen and D. J Tildesley, *Computer Simulation of Liquids* (Clarendon, Oxford, 1987).

[61] J. M. Hartmann, C. Boulet, H. Tran, and M. T. Nguyen, J. Chem. Phys. **133**, 144313 (2010).

[62] L. R. Fokin and A. N. Kalashnikov, High temperature **46**, 614 (2008).

[63] J. M. Hartmann and C. Boulet, "Quantum and classical approaches for rotational relaxation and nonresonant laser alignment of linear molecules. A comparison for CO_2 gas in the nonadiabatic regime," J. Chem. Phys. (to be published).